British Journal of Pharmacology (2008) 153, 380–389
 0007–1188/08 $30.00
www.brjpharmacol.org

RESEARCH PAPER

Compartmentalization of endocannabinoids into lipid rafts in a dorsal root ganglion cell line

N Rimmerman, HV Hughes, HB Bradshaw, MX Pazos, K Mackie, AL Prieto and JM Walker

Department of Psychological and Brain Sciences and the Gill Center for Biomolecular Sciences, Indiana University, Bloomington, IN, USA

Background and purpose: *N*-arachidonoyl ethanolamine (AEA) and 2-arachidonoyl glycerol (2-AG) are endogenous cannabinoids binding to the cannabinoid receptors CB_1 and CB_2 to modulate neuronal excitability and synaptic transmission in primary afferent neurons. To investigate the compartmentalization of the machinery for AEA and 2-AG signalling, we studied their partitioning into lipid raft fractions isolated from a dorsal root ganglion X neuroblastoma cell line (F-11).
Experimental approach: F-11 cells were homogenized and fractionated using a detergent-free OptiPrep density gradient. All lipids were partially purified from methanolic extracts of the fractions on solid phase cartridges and quantified using liquid chromatography tandem mass spectrometry (LC/MS/MS). Protein distribution was determined by Western blotting.
Key results: Under basal conditions, the endogenous cannabinoid AEA was present in both lipid raft and specific non-lipid raft fractions as was one of its biosynthetic enzymes, NAPE-PLD. The 2-AG precursor 1-stearoyl-2-arachidonoyl-*sn*-glycerol (DAG), diacylglycerol lipase α (DAGLα), which cleaves DAG to form 2-AG, and 2-AG were all co-localized with lipid raft markers. CB_1 receptors, previously reported to partition into lipid raft fractions, were not detected in F-11 membranes, but CB_2 receptors were detected at high levels and partitioned into non-lipid raft fractions.
Conclusions and implications: The biochemical machinery for the production of 2-AG via the putative diacylglycerol pathway is localized within lipid rafts, suggesting that 2-AG synthesis via DAG occurs within these microdomains. The observed co-localization of AEA, 2-AG, and their synthetic enzymes with the reported localization of CB_1 raises the possibility of intrinsic-autocrine signalling within lipid raft domains and/or retrograde-paracrine signalling.
British Journal of Pharmacology (2008) **153,** 380–389; doi:10.1038/sj.bjp.0707561; published online 29 October 2007

Keywords: cannabinoid; lipid raft; dorsal root ganglia; diacylglycerol; CB_2; caveolae; electrospray ionization mass spectrometry

Abbreviations: 2-AG, 2-arachidonoyl glycerol; AEA, *N*-arachidonoyl ethanolamine; AMT, AEA transporter; DAG, diacylglycerol; DAGLα, diacylglycerol lipase α; GPI, glycosylphosphatidylinositol; LC/MS/MS, liquid chromatography tandem mass spectrometry; MBCD, methyl-β cyclodextrins; NAGly, *N*-arachidonoyl glycine; NAPE-PLD, *N*-acyl phosphatidylethanolamine phospholipase D; SSI, self-induced slow long-lasting inhibition

Introduction

Lipid rafts are specialized membrane domains enriched in cholesterol, sphingolipids and glycosphingolipids compared with the phospholipid-rich surrounding membranes. These domains are involved in several functions including intracellular signalling, cellular polarity, molecule sorting and membrane transport (Moffett *et al*., 2000; Gaus *et al*., 2003; Chini and Parenti, 2004; Wilson *et al*., 2004). Caveolae, a lipid raft subtype containing proteins such as caveolins and flotillins, were explored as a compartmentalization site for endocannabinoid signalling including the endocannabinoid *N*-arachidonoyl ethanolamine (AEA) and its target, the cannabinoid CB_1 receptor (Fielding and Fielding, 1997; Czarny *et al*., 1999; Keren and Sarne, 2003; McFarland *et al*., 2004; Rajendran *et al*., 2007).

The partitioning of CB_1 receptors into specialized membrane domains was postulated from a C-terminal palmitoylation domain required for proper interactions with lipid raft-associated G proteins (for reviews see Mukhopadhyay *et al*., 1999; Barnett-Norris *et al*., 2005; Fay *et al*., 2005; Xie and Chen, 2005). Keren and Sarne (2003) reported that internalization of CB_1 receptors in HEK293-CB_1 transfected cells occurred via both clathrin-coated pits and caveolae, although the latter was absent in N18TG2 neuroblastoma cells natively expressing CB_1 receptors or CB_1 transfected AtT20 cells (Hsieh *et al*., 1999). Bari *et al*. (2005a, b) showed that in rat C6 glioma cells, CB_1 receptor binding and signalling were doubled following lipid raft disruption by cholesterol depletion with methyl-β cyclodextrins, while cholesterol enrichment of C6 glioma cells led to reduced CB_1

Correspondence: Professor JM Walker, Psychological and Brain Sciences, Indiana University, 1101 East 10th Street, Bloomington, IN 47405, USA.
E-mail: walkerjm@indiana.edu
Received 5 July 2007; revised 18 September 2007; accepted 5 October 2007; published online 29 October 2007

receptor binding efficiency. Consistent with these findings, Sarnataro *et al*. (2005, 2006) showed that in MDA-MB-231 breast cancer cells, CB_1 receptors associated with lipid raft fractions and were redistributed mostly to non-lipid raft fractions following treatment with the CB_1 receptor antagonist SR141716A. In contrast to the association of CB_1 receptors with lipid rafts, treatment of CB_2-expressing human DAUDI leukaemia cells with methyl-β cyclodextrins did not affect CB_2 receptor binding or signalling cascades (Bari *et al*., 2006).

Membrane lipid composition may affect endocannabinoid uptake and signalling, thus explaining some of the results described above. Treatment with methyl-β cyclodextrins dose-dependently reduced the uptake of tritiated 2-AG (~50%) in DAUDI cells while cholesterol enrichment increased 2-AG uptake by 175%. The same effect was observed with C6 glioma cells (Bari *et al*., 2006). Similarly, methyl-β cyclodextrins treatment reduced the activity of the putative AEA transporter in rat basophilic leukaemia cells (RBL-2H3; McFarland *et al*., 2004) while a decrease in membrane fluidity induced by cholesterol enrichment increased AEA transporter activity in C6 glioma cells (Bari *et al*., 2005b). Taken together these findings indicate that cholesterol enrichment facilitates endocannabinoid uptake whereas cholesterol depletion reduces endocannabinoid uptake. A contributing factor to this relationship may be the binding affinity of cholesterol to AEA (Biswas *et al*., 2003). These data suggest that the integrity and composition of lipid rafts play a crucial role in endocannabinoid uptake and signalling through cannabinoid receptors.

While it is clear that endocannabinoid signalling is controlled in part by membrane composition, the localization and distribution of endocannabinoids under basal conditions is unknown. In this study, we characterized the membrane compartmentalization of endocannabinoids and their lipid precursors, synthetic enzymes and receptors into domains rich in cholesterol, sphingomyelins, flotillin-1 and caveolin-1 (hereafter referred to as lipid rafts). Although the visualization of lipid rafts in live cells is limited by spatial resolution, membrane dynamics and lipid imaging technology, the unique composition of lipid rafts enables investigation because of their insolubility in non-ionic detergents at 4 °C and buoyancy in density gradients (Macdonald and Pike, 2005; Groves, 2007; Jacobson *et al*., 2007). A recently described detergent-free fractionation method (Macdonald and Pike, 2005) coupled to liquid chromatography/tandem mass spectrometry allowed us to quantify lipid distributions in cell fractions. We report that the biochemical machinery for the production of 2-AG in F-11 cells via the putative diacylglycerol (DAG) pathway is localized within lipid rafts, indicating that 2-AG synthesis from DAG occurs within lipid rafts. We also provide evidence for the production of endocannabinoids outside lipid rafts.

Methods

Cell culture

The DRG X neuroblastoma F-11 cell line was provided by Dr Mark C Fishman, Massachusetts General Hospital (Boston, MA, USA). The F-11 cell line was cultured in Ham's F-12 (1X) with L-glutamine (Mediatech Inc., Herndon, VA, USA) containing 1% penicillin–streptomycin (Invitrogen, Carlsbad, CA, USA), 2% HAT supplement (50 ×; a liquid mixture of sodium hypoxanthine, aminopterin and thymidine; Invitrogen, Carlsbad, CA, USA) and 17% fetal bovine serum. Cells were subcultured every other day using non-enzymatic cell dissociation solution (1 ×; Sigma-Aldrich, St Louis, MO, USA). Cells were grown under 5% CO_2 at 37 °C.

Cell fractionation

Procedures for fractionation were adapted from the method of Macdonald and Pike (2005). Cells were plated 48 h before the experiment. On the day of the experiment, for each condition, cells from five T-150 flasks were washed once with PBS and scraped into a total of 25 ml of 4 °C base buffer (20 mM Tris–HCl, 250 mM sucrose, pH 7.8) containing 1 mM calcium chloride and 1 mM magnesium chloride. Cells were centrifuged in a polystyrene tube at 200 *g* for 7 min at 4 °C. The pellet was re-suspended in 1.0 ml of base buffer containing calcium chloride, magnesium chloride and Complete Protease Inhibitor Cocktail, added at the manufacturer's suggested concentration (Roche, Basel, Switzerland). Cells were then lysed using 20 strokes in a Potter–Elvehjem homogenizer and centrifuged at 1000 *g* for 10 min at 4 °C. The post-nuclear supernatant was transferred to a new tube, the pellet was re-suspended in base buffer containing calcium chloride, magnesium chloride and protease inhibitors, and the procedure was repeated. The 2 ml of post-nuclear supernatants obtained were combined and 50% OptiPrep (Axis Shield, Dundee, UK) in base buffer was added to give a 4 ml solution of 25% OptiPrep. This solution was overlaid with an 8 ml continuous density gradient of 20–0% OptiPrep in base buffer in an Ultra-Clear (14 × 89 mm) centrifuge tube. The gradient was centrifuged using an SW-41 swinging bucket rotor (Beckman Coulter, Fullerton, CA, USA) for 90 min at 52 000 *g* at 4 °C. Sixteen fractions of 0.75 ml were collected from each gradient.

Mass spectrometric analysis of lipids

For lipid analysis, 0.6 ml of each fraction was removed and 2 ml of HPLC grade methanol were added. To each sample was added 200 pmol of [$^2H_8$]-*N*-arachidonoyl glycine (NAGly) and HPLC grade water was added to make a 75% aqueous solution. Lipids were extracted as described previously (Bradshaw *et al*., 2006). Briefly, 500 mg C8 Bond Elut solid phase extraction columns (Varian, Harbor City, CA, USA) were conditioned with 5 ml HPLC grade methanol followed by 3.0 ml HPLC water. The 75% aqueous solutions containing the fractions were loaded onto separate columns, which were then washed with 20 ml water. Five sequential elutions (1.5 ml each of 30, 50, 85 and 100% methanol and 100% isopropyl alcohol) were collected for mass spectrometric analysis.

As described previously (Bradshaw *et al*., 2006), sample analysis of lipids was carried out as follows. An aliquot of the eluate was loaded using a Shimadzu SCL10Avp (Wilmington, DE, USA) or an LC Packings Ultimate-3000 (Sunnyvale, CA,

USA) autosampler onto a reversed phase Zorbax 2.1 × 50 mm C8 column maintained at 40 °C. HPLC gradient formation at a flow rate of 200 μl min^{-1} was achieved by a system comprised of a Shimadzu controller and two Shimadzu LC10ADvp pumps or an LC Packings controller and an LPG-3000 loading pump. Lipid levels in the sample were analysed in multiple reaction-monitoring (MRM) mode on a triple quadruple mass spectrometer, either the API 3000 or the API 4000 (Applied Biosystems/MDS SCIEX, Foster City, CA, USA), with electrospray ionization. Methods for lipid analysis were created and optimized by flow injection of lipid standards. All calculations for quantitation experiments (excluding lyso-PI) were based on calibration curves using synthetic standards. The following molecular ion and fragment ion pairs were used to quantify lipids in MRM mode: DAG 1-palmitoyl-2-oleoyl-*sn*-glycerol 595.6→313.3; DAG 1-stearoyl-2-arachidonoyl-*sn*-glycerol 645.7→287.1; cholesterol 404.4→369.3; (24:1)-sphingomyelin 814.8→184.1; (18:0)-sphingomyelin 731.7→184.1; arachidonic acid 303.3→259.3; GM_3 1262.9→290.1; $PGF_{2\alpha}$ 353.3→309.2; PGE_2 351.2→315.0; phosphatidic acids: 1-arachidonoyl-2-plamitoyl-*sn*-glycerol 3-phosphate 719.5→621.3/ 719.5→599.6, 1-arachidonoyl-2-stearoyl-*sn*-glycerol 3-phosphate 747.4→649.6; 2-AG 379.3→287.3; AEA 348.2→62.1; *N*-palmitoyl ethanolamine 300.2→62.1; phosphatidyl inositol 885.6→303.3, 885.6→241.0, 885.6→283.3; lyso-phosphatidyl inositol 619.6→303.3, 619.6→241.2.

Protein assay

Protein levels in each fraction were determined using the DC Protein Assay kit from Bio-Rad Laboratories (Hercules, CA, USA). The absorbance of samples following reaction was measured at 595 nm using a SpectraMax M5 spectrophotometer from Molecular Devices (Sunnyvale, CA, USA). Optical densities were transformed using an albumin standard curve. The transformed values from fractions of a control OptiPrep gradient lacking cell lysate were subtracted from corresponding fractions containing cell lysate to adjust for cross reactivity between OptiPrep and the protein assay reagents and determine actual protein levels in each fraction.

Western blot analysis

Membrane components present in the gradient fractions were lysed by the addition of 0.5% SDS (Sigma-Aldrich, St Louis, MO, USA), 1% NP-40 (EMD Biosciences Inc., La Jolla, CA, USA) and 1% Triton X-100 (Sigma-Aldrich, St Louis, MO, USA). Samples were incubated on ice for 30 min. Loading buffer was added to the samples to achieve final concentrations of 0.1 M Tris (pH 6.8), 10% glycerol, 0.1% bromophenol blue, 2% SDS and 5% β-mercaptoethanol. Samples were denatured for 3 min at 98 °C using a Fisher Scientific 2001FS hot plate (Fisher Scientific, Hampton, NH, USA) and cold spun for 3 min on a Hettich Mikro 22R microcentrifuge (Hettich, Germany) before loading onto a Novex Tris-glycine 4–20% gel (Invitrogen, Carlsbad, CA, USA). A chemiluminescent BlueRanger molecular weight marker (Pierce, Rockford, IL, USA) containing seven protein markers in the range 18–220 kDa was loaded for each membrane. Protein separation was carried out at 200 V using a PowerPac HC power supply (Bio-Rad, Hercules, CA, USA) and an XCell Sure Lock mini cell apparatus (Invitrogen, Carlsbad, CA, USA). Proteins were transferred from the gel onto Immobilon P membranes (Millipore, Billerica, MA, USA) through electrophoretic transfer using a GENIE (Idea Scientific Company, Minneapolis, MN, USA). The membranes were blocked in blocking buffer consisting of TBST (10 mM Tris–HCl (pH 7.5), 150 mM NaCl and 0.1% Tween 20) with 3% w/v skim milk (Carnation, Nestle, Vevey, Switzerland). The membranes were incubated overnight at 4 °C in the presence of primary antibody or antibody + blocking peptide on a Roto Mix orbital shaker (Barnstead/Thermolyne, Dubuque, IA, USA). The following affinity-purified antibodies were used for the western blot analyses: anti-flotillin (1:250 dilution), anti-caveolin (1:1000 dilution), anti-neuronal NO synthase, (1:2500 dilution), anti-CB_2 (1:500–1000 dilution), anti-NAPE PLD (1: 500 dilution), anti-DGL-α (1:1000–2000 dilution).

The membranes were washed five times for 5 min per wash with TBST, blocked for 15 min as described above and then incubated 60–180 min with either HRP-goat anti-rabbit IgG or HRP-goat anti-mouse IgG (1:10 000 dilution) on a Roto Mix orbital shaker. The blots were washed five times for 5 min per wash with TBST and processed using chemiluminescent detection using the Super Signal West Pico Chemiluminescent Substrate ECL system (Pierce, Rockford, IL, USA) according to instructions provided by the manufacturers. The chemiluminescent images were acquired using a Kodak 2000R image station (Kodak, Rochester, NY, USA). Western blots were repeated a minimum of three times per protein tested.

Statistical analysis

Differences in lipid levels were assessed by one-way analysis of variance (ANOVA) with Fisher's LSD *post hoc* test (SPSS, Chicago, IL, USA). Differences were considered significant for *P*-values less than 0.05. Data are shown as mean ± s.e. mean.

Reagents for mass spectrometry and HPLC

[$^2H_8$]-*N*-arachidonoyl glycine ([$^2H_8$]-NAGly), [$^2H_8$]-*N*-arachidonoyl ethanolamine ([$^2H_8$]-AEA), AEA, NAGly, palmitoyl ethanolamine, arachidonic acid, [$^2H_8$]-arachidonic acid, prostaglandin PGE_2, $PGF_{2\alpha}$ and 2-AG were purchased from Cayman Chemical (Ann Arbor, MI, USA). Diacylglycerols (DAGs), phosphatidic acids, cholesterol, phosphatidyl inositol (PI) and lyso-PI were purchased from Avanti Polar Lipids Inc., (Alabaster, AL, USA). GM_3 was purchased from Sigma-Aldrich (St Louis, MO, USA). High-performance liquid chromatography (HPLC) grade methanol, acetonitrile and isopropyl alcohol were purchased from VWR international (Plainview, NY, USA) and HPLC grade water was obtained using a MilliQ Gradient apparatus from Millipore (Milford, MA, USA). HPLC grade acetic acid and ammonium acetate were purchased from Sigma-Aldrich (St Louis, MO, USA).

Antibodies

Affinity purified rabbit polyclonal antibodies to: L15-CB_1 receptor, CT_t-CB_2 receptor, *N*-acyl phosphatidylethanolamine phospholipase D (NAPE-PLD) and diacylglycerol lipase

α (DGLα) were used with their respective blocking peptides (Katona *et al*., 2006; Leung *et al*., 2006). The specificity of the CB_2-CTt antibody was tested by staining spleen sections from CB_2 (−/−) and wild-type mice (data not shown). The immunizing proteins for each antibody: CB_2- CTt, NAPE-PLD and DGLα completely blocked the corresponding bands at 45, 46 and 115 kDa, respectively. The fatty acid amide hydrolase rabbit polyclonal antibody was purchased from Cayman Chemical (Ann Arbor, MI, USA). Rabbit polyclonal antibody for caveolin-1 was purchased from Cell Signalling Technology (Danvers, MA, USA). Antibodies to mouse neuronal NO synthase and mouse flotillin-1 were purchased from BD Transduction Laboratories (San Diego, CA, USA).

Results

Localization of lipid raft markers

Fractions 10–12 of the cell fractionation gradient contained lipid rafts as assessed by the colocalization of lipid raft associated proteins caveolin-1 and flotillin-1 with high levels of cholesterol, sphingomyelins and the glycosphingolipid ganglioside GM_3 in these fractions (Figures 1 and 2a). The protein distribution within the gradient fractions was also assessed, with high-protein levels detected in fractions 1–6 as well as the low-density fractions 10–12 (Figure 2b).

Localization of AEA and its metabolite arachidonic acid under basal conditions or following exogenous administration of [$^2H_8$]-AEA

Under basal conditions the levels of endogenous AEA peaked in non-lipid raft fraction 6 as well as lipid raft fraction 10, and the more abundant *N*-palmitoyl ethanolamine showed a similar trend (Figure 3b). A synthetic enzyme for *N*-acyl ethanolamine production, *N*-acyl phosphatidylethanolamine phospholipase D (NAPE-PLD), was similarly distributed among lipid raft fractions 10–11 and non-lipid raft fraction 6 (Figure 1).

To test the cellular localization of exogenously delivered AEA, we applied deuterium-labelled AEA to F-11 cells. Following incubation with 5 μM [$^2H_8$]-AEA at 37 °C for 1 h prior to the fractionation procedure, the distribution of [$^2H_8$]-AEA resembled the distribution of endogenous AEA, with significantly higher levels in fractions 5 and 10 compared to other fractions. [$^2H_8$]-Arachidonic acid, a metabolite of [$^2H_8$]-AEA, was localized mostly to non-lipid raft fractions with levels being highest in fraction 5 (Figure 3c). Additionally, native arachidonic acid colocalized with its endogenous cyclooxygenase metabolites prostaglandin E_2 and prostaglandin $F_{2\alpha}$ in non-lipid raft fractions 1–6 (Figure 3a).

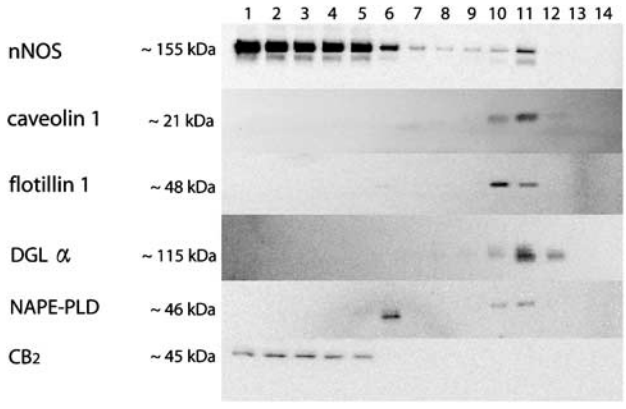

Figure 1 Distribution of protein lipid raft markers across F-11 fractions. The lipid raft markers caveolin-1 and flotillin-1 were concentrated in lipid raft fractions 10–11. Neuronal NO synthase was spread across lipid raft and non-lipid raft fractions. *N*-acyl phosphatidylethanolamine phospholipase D was highest in fraction 6 and elevated in fractions 11–12. Cannabinoid CB_2 receptors were localized to non-lipid raft fractions 1–5. The enzyme diacylglycerol lipase α was localized to lipid raft fractions 10–12. Blots are representative of three blots per protein.

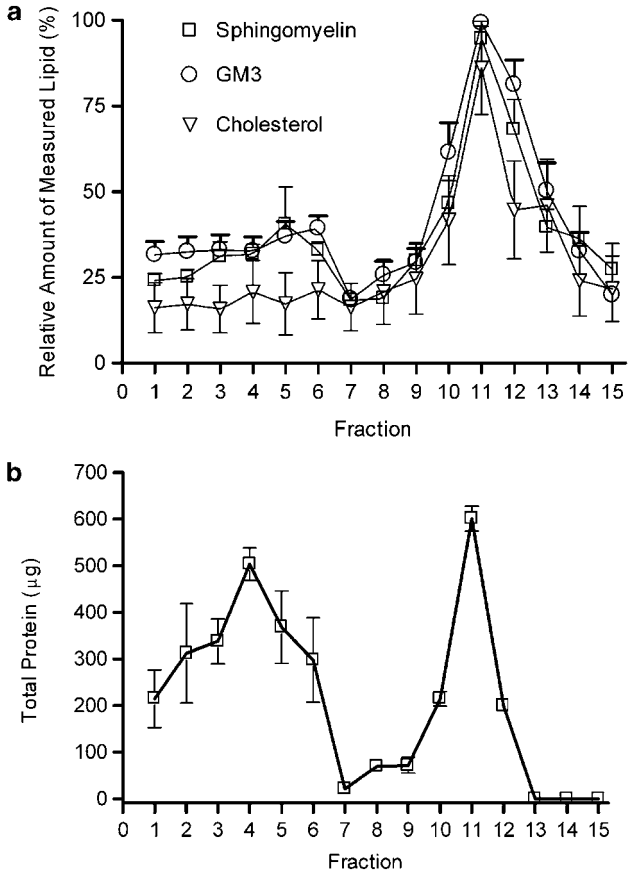

Figure 2 (**a**) Distribution of lipid molecule lipid raft markers. Lipids are presented as a percent of the highest fraction in each fractionation experiment. Cholesterol was significantly higher in fractions 10–13, $P<0.05$, $n=7$, one-way ANOVA with Fisher's LSD *post hoc*. The glycosphingolipid ganglioside M_3 (GM_3) was significantly higher in fractions 10–12 compared with all other fractions $P<0.001$, ($n=7$). The levels in these fractions were also significantly different from each other, $P<0.005$, one-way ANOVA with Fisher's LSD *post hoc*. Sphingomyelin (18:0) was highest in fractions 11–12, $P<0.05$, $n=4$, one-way ANOVA with Fisher's LSD *post hoc*. (**b**) Distribution of total proteins in fractions. Total protein levels were highest in lipid raft fraction 11 and non-lipid raft fraction 4. Protein levels were low in fractions 7–9 and were below our detection limit in fractions 13–16. Error bars represent s.e.mean.

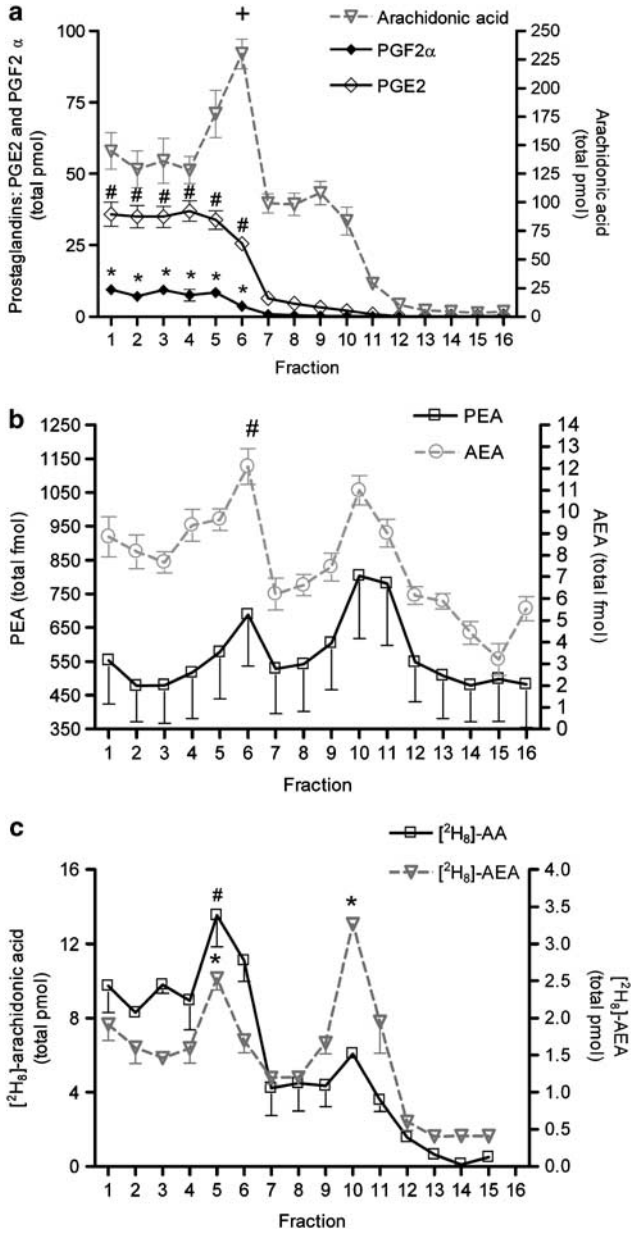

Figure 3 (**a**) Distribution of free arachidonic acid and prostaglandins. Fraction 6 contained the highest levels of arachidonic acid ($n=6$; $^{+}P<0.005$, one-way ANOVA, Fisher's LSD *post hoc*). Its prostaglandin metabolites, PGE_2 and $PGF_{2\alpha}$ were highest in fractions 1–6 where they were significantly elevated compared to lipid raft fractions 10–13 ($n=6$–7; PGE_2, $^{\#}P<0.001$; $PGF_{2\alpha}$ $^{*}P<0.01$: one-way ANOVA, Fisher's LSD *post hoc*). Data are presented as the total quantity in pmol recovered from 600 μl of each fraction. Error bars represent s.e. mean. (**b**) Distribution of acyl ethanolamines. AEA was significantly higher in fraction 6 compared with all fractions except for lipid raft fraction 10, $n=12$, $^{\#}P<0.05$, one-way ANOVA, Fisher's LSD *post hoc*. Palmitoyl ethanolamine (PEA) showed a trend similar to AEA. However, no significant differences were observed in the distribution of PEA between fractions. Data are presented as the quantity in fmol recovered from 600 μl of each fraction. (**c**) Distribution of exogenously administered $[^2H_8]$-AEA and its metabolite $[^2H_8]$-arachidonic acid. $[^2H_8]$-AEA was significantly higher in fractions 10 ($P<0.01$, $n=3$) and 5 ($^{*}P<0.05$, $n=3$) compared with all other fractions, one-way ANOVA, Fisher's LSD *post hoc*. Levels of its metabolite $[^2H_8]$-arachidonic acid were highest in fraction 5 ($^{\#}P<0.05$, excluding fraction 6, $n=3$). Data are presented as the total quantity in pmol recovered from 600 μl of each fraction. Error bars represent s.e. mean.

Localization of 2-AG and its putative precursors under basal conditions

The endocannabinoid 2-AG was primarily found in lipid raft fractions 10–11, its levels being significantly higher than in any other fraction. In the non-lipid raft fraction 6, levels of 2-AG were about 50% of those found in lipid raft fractions 10–11 (Figure 4a). A major pathway for 2-AG synthesis occurs through the cleavage of 2-arachidonoyl diacylglycerols (2-arachidonoyl DAG) by the enzyme DAGLα, (Stella *et al*., 1997; Bisogno *et al*., 2003). To investigate the cellular dynamics of 2-AG biosynthesis, the partitioning of two diacylglycerols (1-stearoyl-2-arachidonoyl-*sn*-glycerol and 1-palmitoyl-2-oleoyl-*sn*-glycerol) and DAGLα, in lipid rafts were compared.

1-Stearoyl-2-arachidonoyl-*sn*-glycerol, a putative precursor of 2-AG, but not 1-palmitoyl-2-oleoyl-*sn*-glycerol, was localized to lipid rafts (Figures 4a and b). The higher levels of 2-arachidonoyl-DAG and 2-AG in lipid raft fractions correlated with the distribution of the enzyme DGLα (Figure 1) in the same fractions.

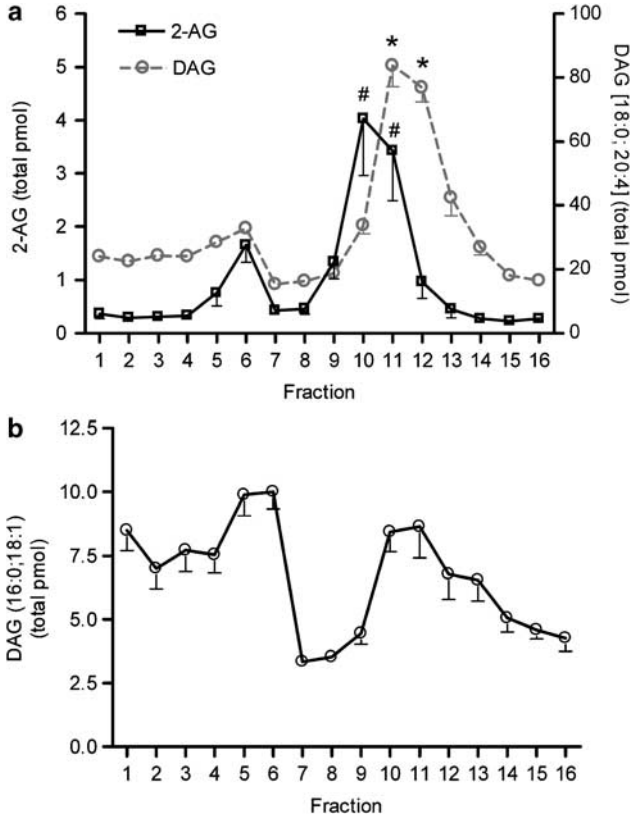

Figure 4 (**a**) Distribution of 2-AG and its putative DAG precursor. 2-AG (left *y* axis, squares) was significantly higher in lipid raft fractions 10–11 ($^{\#}P<0.001$; $n=8$, one-way ANOVA, Fisher's LSD *post hoc*). Arachidonoyl-containing DAG (1-stearoyl-2-arachidonoyl *sn*-glycerol) was most abundant in fractions 11–12 ($^{*}P<0.0001$, $n=7$, one-way ANOVA, Fisher's LSD *post hoc*). Data are presented as the total quantity in pmol recovered from 600 μl of each fraction. (**b**) The distribution of a DAG lacking arachidonoyl chains. There were no significant differences between levels of DAG (1-palmitoyl-2-oleoyl *sn*-glycerol) in the cell fractions. Error bars represent s.e. mean.

Two main routes for the production of arachidonoyl-containing DAGs have been proposed. Bisogno *et al.* (1999) reported the production of DAGs from phosphatidic acid. This route was observed in N18TG2 cells upon stimulation with ionomycin. A second pathway involves phospholipase C-mediated synthesis of DAGs from phosphatidylinositol, a phospholipid that often contains the arachidonoyl moiety at the sn-2 position (Prescott and Majerus, 1981, 1983; Sugiura *et al.*, 1995, 2006; Kondo *et al.*, 1998). This pathway was first observed in platelets following stimulation with thrombin.

We measured two species of arachidonoyl-containing phosphatidic acids (1-palmitoyl-2-arachidonoyl-*sn*-glycerol-3-phosphate and 1-stearoyl-2-arachidonoyl-*sn*-glycerol-3-phosphate) as well as arachidonoyl-containing PI. Both phosphatidic acids as well as arachidonoyl-containing PI were significantly higher in non-lipid raft fractions (Figures 5a and b). An additional pathway for the production of 2-AG from lyso-PI via the enzyme lyso-PI-specific PLC was reported in rat brain synaptosomal fractions, suggesting a localization of this pathway in synapses (Ueda *et al.*, 1993; Tsutsumi *et al.*, 1994). In this study, levels of 2-arachidonoyl lyso-PI were also found to be higher in non-lipid raft fractions (Figure 5a).

Patterns of the distribution of AEA and 2-AG as well as their related enzymatic machinery in F-11 fractions led us to examine the distribution of their targets, the cannabinoid receptors. The CB_1 receptor protein was below our detection limit by Western blotting. However, the CB_2 receptor was localized to non-lipid raft fractions 1–5 (Figure 1).

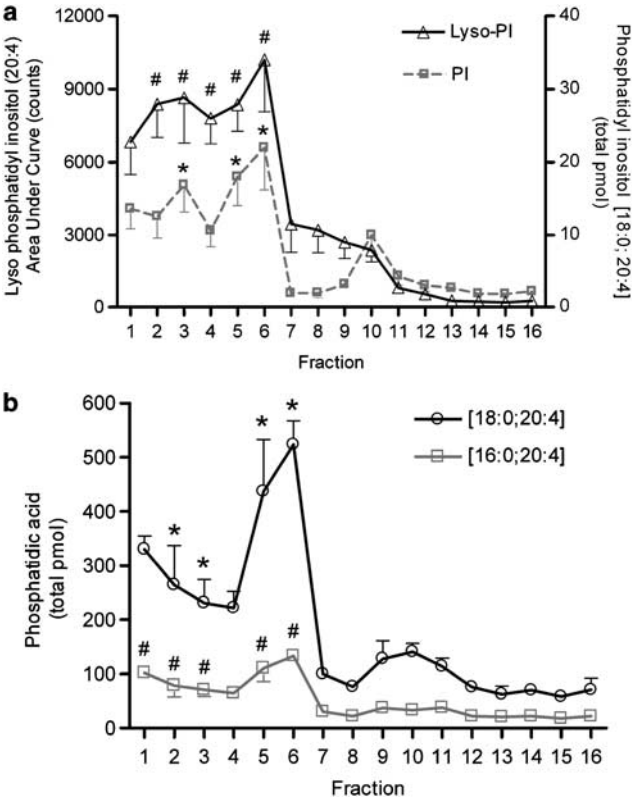

Figure 5 (**a**) Distribution of arachidonoyl-containing lyso-phosphatidyl inositol (lyso-PI) and PI. The arachidonoyl-containing lyso-PI was highest in fractions 2–6 where the levels were significantly different from fractions 7–16 ($^{\#}P<0.005$, $n=6$, one-way ANOVA, Fisher's LSD *post hoc*). The highest levels of the arachidonoyl-containing phosphatidyl inositol (18:0; 20:4) were found in fractions 3 and 5–6, which significantly differed from fractions 7–16 in PI levels ($^{*}P<0.05$, $n=6$, one-way ANOVA, Fisher's LSD *post hoc*). Data for PI are presented as the total quantity in pmol recovered from 600 μl of each fraction. Due to the absence of a synthetic standard for lyso-PI (20:4), data are presented as integrated area under the curve in counts. (**b**) Distribution of arachidonoyl-containing phosphatidic acids. The levels of arachidonoyl-containing phosphatidic acid 1-palmitoyl-2-arachidonoyl *sn*-glycerol-3-phosphate were highest in fractions 1–3 and 5–6 and were significantly different from fractions 7–16 ($^{\#}P<0.05$, $n=3$–5, one-way ANOVA, Fisher's LSD *post hoc*). The highest levels of the arachidonoyl-containing phosphatidic acid 1-stearoyl-2-arachidonoyl-*sn*-glycerol-3-phosphate were found in fractions 1–2 and 5–6 and were significantly different from fractions 7–16 ($^{*}P<0.05$, $n=3$–5, one-way ANOVA, Fisher's LSD *post hoc*).

Discussion

Lipid rafts have emerged as important domains for the assembly of signalling machinery, serving key roles in several signal transduction cascades. Here, we examined the localization of endocannabinoid signalling components to lipid-raft and non-lipid raft fractions in F-11 cells, a cell line created by the fusion of rat embryonic (days 13–14) dorsal root ganglion cells and mouse N18TG2 neuroblastoma cells. F-11 cells exhibit characteristics of sensory neurons and express several lipid-activated receptors, including the cannabinoid CB_1 and CB_2 receptors (Ross *et al.*, 2001), transient receptor potential vanilloid type-2 channels and PG receptors (Francel *et al.*, 1987; Smith *et al.*, 1998; Jahnel *et al.*, 2003; Bender *et al.*, 2005). In addition, these cells produce numerous signalling lipids including gangliosides, arachidonoyl-containing DAGs, PI and lyso-PI (Francel and Dawson, 1988; Ariga *et al.*, 1995; Zeng *et al.*, 2000).

Localization of N-arachidonoyl ethanolamine and NAPE-PLD

There are several pathways for the production of AEA (Di Marzo *et al.*, 1994; Kurahashi *et al.*, 1997; Hansen *et al.*, 2000a, b; Schmid *et al.*, 2002; Okamoto *et al.*, 2004; Sun *et al.*, 2004; Morishita *et al.*, 2005; Leung *et al.*, 2006; Liu *et al.*, 2006). A major pathway for the production of *N*-acyl ethanolamines occurs through the cleavage of *N*-acyl phosphatidylethanolamine (NAPE) via the enzyme *N*-acyl phosphatidylethanolamine-hydrolysing phospholipase D (NAPE-PLD; Di Marzo *et al.*, 1994; Schmid, 2000; Hansen *et al.*, 2000a, b; Okamoto *et al.*, 2004; Morishita *et al.*, 2005). NAPE-PLD is a membrane bound 46 kDa protein that belongs to the zinc-metallo-hydrolase family of the β-lactamase fold and does not resemble other known PLDs (Daiyasu *et al.*, 2001; Ueda *et al.*, 2005). In our preparations, the distribution of basal levels of endogenous AEA and NAPE-PLD mirrored one another in both lipid raft and non-lipid raft fractions, possibly due to increased production of AEA in compartments with higher levels of its synthetic enzyme. The mixed distribution may imply trafficking of the enzyme into different compartments both within and outside lipid rafts as reported previously for other proteins. Such activity may be induced by protein co- or post-translational modifications, including glycosylphosphatidylinositol-anchoring,

cholesterol binding, or acylation (Pechlivanis and Kuhlmann, 2006). The specifics of such regulation of NAPE-PLD remain to be investigated.

To further investigate compartmentalization of the molecules involved in AEA metabolism, we examined the localization of deuterated arachidonic acid derived from the breakdown of exogenously administered deuterated AEA. Deuterated arachidonic acid colocalized mostly with non-lipid raft fractions, consistent with a report on the localization of fatty acid amide hydrolase to non-lipid raft membranes (McFarland *et al*., 2004). Furthermore, the finding that both native arachidonic acid and its cyclooxygenase-2 metabolites, the PGs, are localized to non-lipid raft fractions suggests that metabolism of AEA through cyclooxygenase-2 may also occur in non-lipid raft domains of the membrane. The localization of PGE_2 ethanolamide, a major cyclooxygenase-2 metabolite of AEA (Yu *et al*., 1997), as well as other prostanoid metabolites of AEA in these non-lipid raft fractions will have to be addressed in future studies.

Data from this study together with previous research suggest that some aspects of AEA metabolism, both synthesis by NAPE-PLD and degradation through fatty acid amide hydrolase or cyclooxygenase-2, are localized to specific non-lipid raft regions of the membrane. Furthermore, the finding that exogenously administered deuterated AEA localized to lipid rafts is consistent with the lipid raft-mediated endocytosis of AEA, a hypothesis proposed by McFarland *et al*. (2004).

Localization of 2-arachidonoyl glycerol, DGLα and diacylglycerol

There are several pathways through which cells may synthesize 2-AG. One pathway involves hydrolysis of arachidonoyl-containing DAG through the (*sn*-1) diacylglycerol lipase enzymes (Prescott and Majerus, 1981, 1983; Stella *et al*., 1997; Bisogno *et al*., 1999). Our experiments showed that endogenous 2-AG is concentrated in lipid raft fractions, where it colocalized with DGLα and an arachidonoyl-containing DAG.

The distribution of another DAG lacking an arachidonoyl moiety and hence not a 2-AG precursor was also examined. This DAG was localized to both lipid raft and non-lipid raft fractions, unlike the arachidonoyl containing DAG. DGLα had no selectivity for substrate acyl chain length or saturation (Sugiura *et al*., 1995; Bisogno *et al*., 2003). Thus, the selective trafficking of arachidonoyl-containing DAG to lipid rafts may be crucial for the selective enhancement of 2-AG production in lipid rafts by DGLα. Taken together, these findings indicate that lipid rafts may serve as platforms for the clustering of components of the diacylglycerol pathway for 2-AG production.

The role of membrane compartmentalization in endocannabinoid signalling

Endocannabinoid signalling has been implicated in processes affecting synaptic plasticity, with physiological and anatomical studies supporting the idea of paracrine endocannabinoid signalling. 2-AG is a key player in endocannabinoid-induced synaptic modulation in the nervous system. It was hypothesized to be synthesized in the postsynaptic membrane in a calcium-dependent fashion following depolarization or activation of G protein-coupled receptors such as group-I metabotropic receptors (Bisogno *et al*., 1997; Stella *et al*., 1997; Varma *et al*., 2001; Straiker and Mackie, 2007). 2-AG may then travel in a retrograde manner to activate presynaptic CB_1 receptors leading to inhibition of neurotransmitter release in the short-term plasticity phenomena of depolarization-induced suppression of inhibition or excitation and metabotropic suppression of inhibition or excitation, as well as long-term depression (Varma *et al*., 2001; Wilson *et al*., 2001; Chevaleyre and Castillo, 2003; Freund *et al*., 2003; Safo and Regehr, 2005; Straiker and Mackie, 2007). Support for this hypothesis comes from the discovery that DGLα is localized specifically to the perisynaptic annulus around the postsynaptic density of excitatory synapses receiving asymmetrical contacts from presynaptic CB_1 receptor-expressing axon terminals (Katona *et al*., 2006; Yoshida *et al*., 2006). Additionally, it was shown that DGLα interactions with scaffold proteins (Homer 1b, Homer-2) may modulate its plasma membrane association (Jung *et al*., 2007).

An obstacle for the theory of retrograde transport of 2-AG has been in identifying a mechanism for the movement of 2-AG, a hydrophobic molecule, through the aqueous medium of the synaptic cleft. A possible mechanism may be the incorporation of 2-AG into exosomes, microvesicles of endosomal origin that are released into the extracellular matrix and participate in intercellular cargo exchange (Faure *et al*., 2006). It was recently shown that exosomes are released upon cellular stimulation from cortical neurons and, like lipid rafts, they contain flotillin-1, glycosylphosphatidylinositol-anchored proteins and high levels of cholesterol (de Gassart *et al*., 2003; Wubbolts *et al*., 2003). Thus, a rise in DGLα activity upon stimulation of the postsynaptic neuron may lead to increased production of 2-AG in lipid rafts, followed by the release of 2-AG-rich exosomes pinched off from lipid rafts. The fusion of exosomes with the presynaptic membrane may serve to deliver 2-AG to activate CB_1 receptors. Although the similarities in composition of lipid rafts and exosomes support this hypothesis, further investigation will be needed to examine the possibility that exosomes originate from lipid rafts.

Paracrine signalling may not be the only mechanism through which endocannabinoids signal. Data from this study suggest that autocrine signalling of endocannabinoids may occur within lipid rafts. Previous research suggested localization of CB_1 receptors with lipid rafts (Bari *et al*., 2005a) and consistently its colocalization with lipid rafts markers (Sarnataro *et al*., 2005, 2006). In addition, CB_1-receptor distribution was altered by cholesterol depletion, manoeuvres that perturb lipid rafts. In model membrane bilayer systems, AEA was shown to position itself extended with its head group proximal to the polar phospholipid head groups and with its acyl chain parallel to those of the phospholipids in the bilayer (Lynch and Reggio, 2005, 2006; Tian *et al*., 2005). It was suggested that this orientation would facilitate movement to the receptor through fast lateral diffusion (Makriyannis *et al*., 2005). The observation

here that AEA and NAPE-PLD are concentrated in lipid raft fractions along with previously reported localization of CB_1 receptors to lipid rafts suggests that AEA may be produced in lipid rafts whereupon it could rapidly move to nearby CB_1 receptors. Similarly, lipid rafts may also be involved in specifying 2-AG's interactions with its receptors. The close proximity of the synthetic enzymes for 2-AG, 2-AG itself and CB_1 receptors indicates that as with AEA, 2-AG is likely to be produced in lipid rafts and to move rapidly to nearby CB_1 receptors. These data extend previous observations suggesting autocrine actions of endocannabinoids. A physiological example of this autocrine action is self-induced slow long-lasting inhibition (SSI). SSI is a sustained hyperpolarization seen in certain CB_1 receptor-expressing cortical interneurons following a burst of action potentials (Bacci *et al*., 2004). The antagonism of SSI by AM251 and intracellular BAPTA plus its mimicking by exogenously applied 2-AG suggest that it is mediated by CB_1 receptors. Our results indicate that the endocannabinoids 2-AG and AEA, along with the cellular machinery for their synthesis and binding are localized in a manner that would facilitate their role as autocrine ligands for CB_1 receptors, as suggested for SSI. By contrast, our findings indicate that CB_2 receptors do not colocalize with lipid rafts, which is consistent with the findings of Bari *et al*. (2005a, b, 2006) that cholesterol manipulations affected CB_1 but not CB_2 receptor signalling cascades. This indicates that CB_1 receptors are the likely targets of endocannabinoids synthesized within lipid rafts. In conclusion, the localization of both AEA and 2-AG and the biochemical synthetic machinery for these endocannabinoids within lipid rafts along with the previously observed presence of CB_1 receptors indicates the high likelihood of autocrine actions of the endocannabinoids.

Acknowledgements

We are grateful for the support of the National Institute on Drug Abuse (DA-018224, DA-020402, DA-011322, DA-021696, F32-DA-016825), the Gill Center for Biomolecular Science, Indiana University, Bloomington, and the Lilly Foundation Inc., Indianapolis, IN, USA.

Conflict of interest

The authors state no conflict of interest.

References

Ariga T, Blaine GM, Yoshino H, Dawson G, Kanda T, Zeng GC *et al*. (1995). Glycosphingolipid composition of murine neuroblastoma cells: O-acetylesterase gene downregulates the expression of O-acetylated GD3. *Biochemistry* **34**: 11500–11507.

Bacci A, Huguenard JR, Prince DA (2004). Long-lasting self-inhibition of neocortical interneurons mediated by endocannabinoids. *Nature* **431**: 312–316.

Bari M, Battista N, Fezza F, Finazzi-Agro A, Maccarrone M (2005a). Lipid rafts control signaling of type-1 cannabinoid receptors in neuronal cells. Implications for anandamide-induced apoptosis. *J Biol Chem* **280**: 12212–12220.

Bari M, Paradisi A, Pasquariello N, Maccarrone M (2005b). Cholesterol-dependent modulation of type 1 cannabinoid receptors in nerve cells. *J Neurosci Res* **81**: 275–283.

Bari M, Spagnuolo P, Fezza F, Oddi S, Pasquariello N, Finazzi-Agro A *et al*. (2006). Effect of lipid rafts on Cb2 receptor signaling and 2-arachidonoyl-glycerol metabolism in human immune cells. *J Immunol* **177**: 4971–4980.

Barnett-Norris J, Lynch D, Reggio PH (2005). Lipids, lipid rafts and caveolae: their importance for GPCR signaling and their centrality to the endocannabinoid system. *Life Sci* **77**: 1625–1639.

Bender FL, Mederos YSM, Li Y, Ji A, Weihe E, Gudermann T *et al*. (2005). The temperature-sensitive ion channel TRPV2 is endogenously expressed and functional in the primary sensory cell line F-11. *Cell Physiol Biochem* **15**: 183–194.

Bisogno T, Howell F, Williams G, Minassi A, Cascio MG, Ligresti A *et al*. (2003). Cloning of the first sn1-DAG lipases points to the spatial and temporal regulation of endocannabinoid signaling in the brain. *J Cell Biol* **163**: 463–468.

Bisogno T, Melck D, De Petrocellis L, Di Marzo V (1999). Phosphatidic acid as the biosynthetic precursor of the endocannabinoid 2-arachidonoylglycerol in intact mouse neuroblastoma cells stimulated with ionomycin. *J Neurochem* **72**: 2113–2119.

Bisogno T, Sepe N, De Petrocellis L, Di Marzo V (1997). Biosynthesis of 2-arachidonoyl-glycerol, a novel cannabimimetic eicosanoid, in mouse neuroblastoma cells. *Adv Exp Med Biol* **433**: 201–204.

Biswas KK, Sarker KP, Abeyama K, Kawahara K, Iino S, Otsubo Y *et al*. (2003). Membrane cholesterol but not putative receptors mediates anandamide-induced hepatocyte apoptosis. *Hepatology* **38**: 1167–1177.

Bradshaw HB, Rimmerman N, Krey JF, Walker JM (2006). Sex and hormonal cycle differences in rat brain levels of pain-related cannabimimetic lipid mediators. *Am J Physiol Regul Integr Comp Physiol* **291**: R349–R358.

Chevaleyre V, Castillo PE (2003). Heterosynaptic LTD of hippocampal GABAergic synapses: a novel role of endocannabinoids in regulating excitability. *Neuron* **38**: 461–472.

Chini B, Parenti M (2004). G-protein coupled receptors in lipid rafts and caveolae: how, when and why do they go there? *J Mol Endocrinol* **32**: 325–338.

Czarny M, Lavie Y, Fiucci G, Liscovitch M (1999). Localization of phospholipase D in detergent-insoluble, caveolin-rich membrane domains. Modulation by caveolin-1 expression and caveolin-182-101. *J Biol Chem* **274**: 2717–2724.

Daiyasu H, Osaka K, Ishino Y, Toh H (2001). Expansion of the zinc metallo-hydrolase family of the beta-lactamase fold. *FEBS Lett* **503**: 1–6.

de Gassart A, Geminard C, Fevrier B, Raposo G, Vidal M (2003). Lipid raft-associated protein sorting in exosomes. *Blood* **102**: 4336–4344.

Di Marzo V, Fontana A, Cadas H, Schinelli S, Cimino G, Schwartz JC *et al*. (1994). Formation and inactivation of endogenous cannabinoid anandamide in central neurons. *Nature* **372**: 686–691.

Faure J, Lachenal G, Court M, Hirrlinger J, Chatellard-Causse C, Blot B *et al*. (2006). Exosomes are released by cultured cortical neurones. *Mol Cell Neurosci* **31**: 642–648.

Fay JF, Dunham TD, Farrens DL (2005). Cysteine residues in the human cannabinoid receptor: only C257 and C264 are required for a functional receptor, and steric bulk at C386 impairs antagonist SR141716A binding. *Biochemistry* **44**: 8757–8769.

Fielding CJ, Fielding PE (1997). Intracellular cholesterol transport. *J Lipid Res* **38**: 1503–1521.

Francel P, Dawson G (1988). Bradykinin induces the bi-phasic production of lysophosphatidyl inositol and diacylglycerol in a dorsal root ganglion X neurotumor hybrid cell line, F-11. *Biochem Biophys Res Commun* **152**: 724–731.

Francel PC, Miller RJ, Dawson G (1987). Modulation of bradykinin-induced inositol trisphosphate release in a novel neuroblastoma x dorsal root ganglion sensory neuron cell line (F-11). *J Neurochem* **48**: 1632–1639.

Freund TF, Katona I, Piomelli D (2003). Role of endogenous cannabinoids in synaptic signaling. *Physiol Rev* **83**: 1017–1066.

Gaus K, Gratton E, Kable EP, Jones AS, Gelissen I, Kritharides L *et al*. (2003). Visualizing lipid structure and raft domains in living cells with two-photon microscopy. *Proc Natl Acad Sci USA* **100**: 15554–15559.

Groves JT (2007). Bending mechanics and molecular organization in biological membranes. *Annu Rev Phys Chem* **58**: 697–717.
Hansen HH, Hansen SH, Schousboe A, Hansen HS (2000a). Determination of the phospholipid precursor of anandamide and other N-acylethanolamine phospholipids before and after sodium azide-induced toxicity in cultured neocortical neurons. *J Neurochem* **75**: 861–871.
Hansen HS, Moesgaard B, Hansen HH, Petersen G (2000b). N-Acylethanolamines and precursor phospholipids - relation to cell injury. *Chem Phys Lipids* **108**: 135–150.
Hsieh C, Brown S, Derleth C, Mackie K (1999). Internalization and recycling of the CB1 cannabinoid receptor. *J Neurochem* **73**: 493–501.
Jacobson K, Mouritsen OG, Anderson RG (2007). Lipid rafts: at a crossroad between cell biology and physics. *Nat Cell Biol* **9**: 7–14.
Jahnel R, Bender O, Munter LM, Dreger M, Gillen C, Hucho F (2003). Dual expression of mouse and rat VRL-1 in the dorsal root ganglion derived cell line F-11 and biochemical analysis of VRL-1 after heterologous expression. *Eur J Biochem* **270**: 4264–4271.
Jung KM, Astarita G, Zhu C, Wallace M, Mackie K, Piomelli D (2007). A key role for diacylglycerol lipase-{alpha} in metabotropic glutamate receptor-dependent endocannabinoid mobilization. *Mol Pharmacol* **72**: 612–621.
Katona I, Urban GM, Wallace M, Ledent C, Jung KM, Piomelli D *et al*. (2006). Molecular composition of the endocannabinoid system at glutamatergic synapses. *J Neurosci* **26**: 5628–5637.
Keren O, Sarne Y (2003). Multiple mechanisms of CB1 cannabinoid receptors regulation. *Brain Res* **980**: 197–205.
Kondo S, Kondo H, Nakane S, Kodaka T, Tokumura A, Waku K *et al*. (1998). 2-Arachidonoylglycerol, an endogenous cannabinoid receptor agonist: identification as one of the major species of monoacylglycerols in various rat tissues, and evidence for its generation through CA2+-dependent and -independent mechanisms. *FEBS Lett* **429**: 152–156.
Kurahashi Y, Ueda N, Suzuki H, Suzuki M, Yamamoto S (1997). Reversible hydrolysis and synthesis of anandamide demonstrated by recombinant rat fatty-acid amide hydrolase. *Biochem Biophys Res Commun* **237**: 512–515.
Leung D, Saghatelian A, Simon GM, Cravatt BF (2006). Inactivation of N-acyl phosphatidylethanolamine phospholipase D reveals multiple mechanisms for the biosynthesis of endocannabinoids. *Biochemistry* **45**: 4720–4726.
Liu J, Wang L, Harvey-White J, Osei-Hyiaman D, Razdan R, Gong Q *et al*. (2006). A biosynthetic pathway for anandamide. *Proc Natl Acad Sci USA* **103**: 13345–13350.
Lynch DL, Reggio PH (2005). Molecular dynamics simulations of the endocannabinoid N-arachidonoylethanolamine (anandamide) in a phospholipid bilayer: probing structure and dynamics. *J Med Chem* **48**: 4824–4833.
Lynch DL, Reggio PH (2006). Cannabinoid CB1 receptor recognition of endocannabinoids via the lipid bilayer: molecular dynamics simulations of CB1 transmembrane helix 6 and anandamide in a phospholipid bilayer. *J Comput Aided Mol Des* **20**: 495–509.
Macdonald JL, Pike LJ (2005). A simplified method for the preparation of detergent-free lipid rafts. *J Lipid Res* **46**: 1061–1067.
Makriyannis A, Tian X, Guo J (2005). How lipophilic cannabinergic ligands reach their receptor sites. *Prostaglandins Other Lipid Mediat* **77**: 210–218.
McFarland MJ, Porter AC, Rakhshan FR, Rawat DS, Gibbs RA, Barker EL (2004). A role for caveolae/lipid rafts in the uptake and recycling of the endogenous cannabinoid anandamide. *J Biol Chem* **279**: 41991–41997.
Moffett S, Brown DA, Linder ME (2000). Lipid-dependent targeting of G proteins into rafts. *J Biol Chem* **275**: 2191–2198.
Morishita J, Okamoto Y, Tsuboi K, Ueno M, Sakamoto H, Maekawa N *et al*. (2005). Regional distribution and age-dependent expression of *N*-acylphosphatidylethanolamine-hydrolyzing phospholipase D in rat brain. *J Neurochem* **94**: 753–762.
Mukhopadhyay S, Cowsik SM, Lynn AM, Welsh WJ, Howlett AC (1999). Regulation of Gi by the CB1 cannabinoid receptor C-terminal juxtamembrane region: structural requirements determined by peptide analysis. *Biochemistry* **38**: 3447–3455.
Okamoto Y, Morishita J, Tsuboi K, Tonai T, Ueda N (2004). Molecular characterization of a phospholipase D generating anandamide and its congeners. *J Biol Chem* **279**: 5298–5305.
Pechlivanis M, Kuhlmann J (2006). Hydrophobic modifications of Ras proteins by isoprenoid groups and fatty acids—More than just membrane anchoring. *Biochim Biophys Acta* **1764**: 1914–1931.
Prescott SM, Majerus PW (1981). The fatty acid composition of phosphatidylinositol from thrombin-stimulated human platelets. *J Biol Chem* **256**: 579–582.
Prescott SM, Majerus PW (1983). Characterization of 1,2-diacylglycerol hydrolysis in human platelets. Demonstration of an arachidonoyl-monoacylglycerol intermediate. *J Biol Chem* **258**: 764–769.
Rajendran L, Le Lay S, Illges H (2007). Raft association and lipid droplet targeting of flotillins are independent of caveolin. *Biol Chem* **388**: 307–314.
Ross RA, Coutts AA, McFarlane SM, Anavi-Goffer S, Irving AJ, Pertwee RG *et al*. (2001). Actions of cannabinoid receptor ligands on rat cultured sensory neurones: implications for antinociception. *Neuropharmacology* **40**: 221–232.
Safo PK, Regehr WG (2005). Endocannabinoids control the induction of cerebellar LTD. *Neuron* **48**: 647–659.
Sarnataro D, Grimaldi C, Pisanti S, Gazzerro P, Laezza C, Zurzolo C *et al*. (2005). Plasma membrane and lysosomal localization of CB1 cannabinoid receptor are dependent on lipid rafts and regulated by anandamide in human breast cancer cells. *FEBS Lett* **579**: 6343–6349.
Sarnataro D, Pisanti S, Santoro A, Gazzerro P, Malfitano AM, Laezza C *et al*. (2006). The cannabinoid CB1 receptor antagonist rimonabant (SR141716) inhibits human breast cancer cell proliferation through a lipid raft-mediated mechanism. *Mol Pharmacol* **70**: 1298–1306.
Schmid HH (2000). Pathways and mechanisms of *N*-acylethanolamine biosynthesis: can anandamide be generated selectively? *Chem Phys Lipids* **108**: 71–87.
Schmid PC, Wold LE, Krebsbach RJ, Berdyshev EV, Schmid HH (2002). Anandamide and other *N*-acylethanolamines in human tumors. *Lipids* **37**: 907–912.
Smith JA, Amagasu SM, Eglen RM, Hunter JC, Bley KR (1998). Characterization of prostanoid receptor-evoked responses in rat sensory neurones. *Br J Pharmacol* **124**: 513–523.
Stella N, Schweitzer P, Piomelli D (1997). A second endogenous cannabinoid that modulates long-term potentiation. *Nature* **388**: 773–778.
Straiker A, Mackie K (2007). Metabotropic suppression of excitation in murine autaptic hippocampal neurons. *J Physiol* **578**: 773–785.
Sugiura T, Kishimoto S, Oka S, Gokoh M (2006). Biochemistry, pharmacology and physiology of 2-arachidonoylglycerol, an endogenous cannabinoid receptor ligand. *Prog Lipid Res* **45**: 405–446.
Sugiura T, Kudo N, Ojima T, Kondo S, Yamashita A, Waku K (1995). Coenzyme A-dependent modification of fatty acyl chains of rat liver membrane phospholipids: possible involvement of ATP-independent acyl-CoA synthesis. *J Lipid Res* **36**: 440–450.
Sun YX, Tsuboi K, Okamoto Y, Tonai T, Murakami M, Kudo I *et al*. (2004). Biosynthesis of anandamide and *N*-palmitoylethanolamine by sequential actions of phospholipase A2 and lysophospholipase D. *Biochem J* **380**: 749–756.
Tian X, Guo J, Yao F, Yang DP, Makriyannis A (2005). The conformation, location, and dynamic properties of the endocannabinoid ligand anandamide in a membrane bilayer. *J Biol Chem* **280**: 29788–29795.
Tsutsumi T, Kobayashi T, Ueda H, Yamauchi E, Watanabe S, Okuyama H (1994). Lysophosphoinositide-specific phospholipase C in rat brain synaptic plasma membranes. *Neurochem Res* **19**: 399–406.
Ueda H, Kobayashi T, Kishimoto M, Tsutsumi T, Okuyama H (1993). A possible pathway of phosphoinositide metabolism through EDTA-insensitive phospholipase A1 followed by lysophosphoinositide-specific phospholipase C in rat brain. *J Neurochem* **61**: 1874–1881.
Ueda N, Okamoto Y, Morishita J (2005). *N*-acylphosphatidylethanolamine-hydrolyzing phospholipase D: a novel enzyme of the beta-lactamase fold family releasing anandamide and other N-acylethanolamines. *Life Sci* **77**: 1750–1758.
Varma N, Carlson GC, Ledent C, Alger BE (2001). Metabotropic glutamate receptors drive the endocannabinoid system in hippocampus. *J Neurosci* **21**: RC188.

Wilson BS, Steinberg SL, Liederman K, Pfeiffer JR, Surviladze Z, Zhang J *et al*. (2004). Markers for detergent-resistant lipid rafts occupy distinct and dynamic domains in native membranes. *Mol Biol Cell* **15**: 2580–2592.

Wilson RI, Kunos G, Nicoll RA (2001). Presynaptic specificity of endocannabinoid signaling in the hippocampus. *Neuron* **31**: 453–462.

Wubbolts R, Leckie RS, Veenhuizen PT, Schwarzmann G, Mobius W, Hoernschemeyer J *et al*. (2003). Proteomic and biochemical analyses of human B cell-derived exosomes. Potential implications for their function and multivesicular body formation. *J Biol Chem* **278**: 10963–10972.

Xie XQ, Chen JZ (2005). NMR structural comparison of the cytoplasmic juxtamembrane domains of G-protein-coupled CB1 and CB2 receptors in membrane mimetic dodecylphosphocholine micelles. *J Biol Chem* **280**: 3605–3612.

Yoshida T, Fukaya M, Uchigashima M, Miura E, Kamiya H, Kano M *et al*. (2006). Localization of diacylglycerol lipase-alpha around postsynaptic spine suggests close proximity between production site of an endocannabinoid, 2-arachidonoyl-glycerol, and presynaptic cannabinoid CB1 receptor. *J Neurosci* **26**: 4740–4751.

Yu M, Ives D, Ramesha CS (1997). Synthesis of prostaglandin E2 ethanolamide from anandamide by cyclooxygenase-2. *J Biol Chem* **272**: 21181–21186.

Zeng G, Gao L, Birkle S, Yu RK (2000). Suppression of ganglioside GD3 expression in a rat F-11 tumor cell line reduces tumor growth, angiogenesis, and vascular endothelial growth factor production. *Cancer Res* **60**: 6670–6676.